

ChemComm

Accepted Manuscript



This is an *Accepted Manuscript*, which has been through the Royal Society of Chemistry peer review process and has been accepted for publication.

Accepted Manuscripts are published online shortly after acceptance, before technical editing, formatting and proof reading. Using this free service, authors can make their results available to the community, in citable form, before we publish the edited article. We will replace this *Accepted Manuscript* with the edited and formatted *Advance Article* as soon as it is available.

You can find more information about *Accepted Manuscripts* in the [Information for Authors](#).

Please note that technical editing may introduce minor changes to the text and/or graphics, which may alter content. The journal's standard [Terms & Conditions](#) and the [Ethical guidelines](#) still apply. In no event shall the Royal Society of Chemistry be held responsible for any errors or omissions in this *Accepted Manuscript* or any consequences arising from the use of any information it contains.

COMMUNICATION

Oxygen adsorption induced surface segregation of titanium oxide by activation in carbon nanofibers for maximizing photocatalytic performance

Cite this: DOI: 10.1039/x0xx00000x

Received 00th January 2015,
Accepted 00th January 2015

DOI: 10.1039/x0xx00000x

www.rsc.org/

Sung-In Lee^{a,b}, Seong-Mu Jo^{a,c}, Han-Ik Joh^{a,c}, Myong-Hoon Lee^b, and Sungho Lee^{a,c}

This research demonstrates a simple method for synthesizing titanium dioxide nanoparticle-decorated carbon nanofibers. These nanofibers showed a highly efficient degradation of methylene blue under UV light because of the synergetic effects of the large surface-active sites of titanium dioxide nanoparticles and the carbon nanofibers on the photocatalytic properties.

Titanium dioxide (TiO₂) has been one of the most widely used metal oxides because of its optical, dielectric, and catalytic properties, which are necessary in various industries that produce dyes, fillers, catalyst supports, and photocatalysts.^{1,2} The photocatalytic properties are of special interest for the neutralization of pollutants and harmful organics. Although TiO₂ nanoparticles were synthesized to maximize their performance by increasing the number of active sites, aggregation of the nanoparticles has limited the effectiveness of the application.³ However, composites have been reported to disperse TiO₂ nanoparticles on substrates, and recently, TiO₂/carbon composites have been attractive because carbonaceous materials can act as thermally stable and electrically conductive substrates.⁴

To prepare TiO₂/carbon composites, TiO₂ nanoparticles were attached to or grown directly on the surface of carbonaceous materials. Kadirova et al. immersed activated carbon felts (ACF), having a surface area of 1,275 m²/g, into TiO₂ nanoparticle-dispersed solutions. After calcining the resulting materials at 250 °C for 1 h, the TiO₂ particles were shown to have aggregated.⁵ During the photo-degradation of methylene blue (MB), ACF/TiO₂ composites and commercial TiO₂ particles degraded 60 and 40%, respectively, of the initial MB concentrations after 2 h.⁵ Another conventional method for synthesizing TiO₂ particles is to grow particles from their precursors using wet chemistry, such as sol-gel reactions. Titanium isopropoxide as a precursor was dissolved in anhydrous ethanol and mixed in the presence of ACF. A subsequent calcination resulted in TiO₂ nanoparticles on the surface of the ACF.

However, TiO₂ nanoparticles uniformly dispersed on the matrix were not successfully synthesized.⁶

This research presents a method for synthesizing well-dispersed TiO₂ nanoparticles on the surface of carbon nanofibers (CNF). As-spun nanofiber webs were prepared by electro-spinning a polyacrylonitrile (PAN)/titanium isopropoxide polymer blend solution. The nanofiber webs were then subjected to an additional heat treatment to provide stabilization, carbonization, and activation. The composite samples were activated for 0, 10, 30, and 60 min and were designated ATCNF0, ATCNF10, ATCNF30, and ATCNF60, respectively.

Scanning electron microscope (SEM) images show that activation does not cause the diameters of the fibers to change significantly (170 to 250 nm). The surface morphology of ATCNF0 does not differ from that of pure, activated CNF (Figure 1a). However, nanoparticles are present on the surface of ATCNF10 and become larger with longer exposure (Figure S1a), which leads to the aggregation of the nanoparticles. The nanoparticles on ATCNF60 range from 30 to 50 nm in diameter (Figure 1b). Most of the nanoparticles in the transmission electron microscope (TEM) images ranged from 5 to 10 nm and are shown to be inside the ATCNF0 fibers, whereas ATCNF60 reveals significant aggregation of the nanoparticles (Figures 1c and d). It is evident that the mild activation under an oxygen atmosphere results in the migration of some of the nanoparticles from the inside to the surface, followed by their growth (Figures 1c-f). More interestingly, selected-area electron diffraction patterns indicate that the nanoparticles in ATCNF0 and ATCNF60 are TiO and TiO₂, respectively.

As the activation time increases, the peaks at 2θ of 37.4°, 43.0°, 62.1°, 74.3°, and 78.1° in X-ray diffractograms (XRD), respectively corresponding to the (111), (200), (220), (113), and (222) planes of TiO, become smaller (Figure 2a). ATCNF30 shows peaks at 2θ of 25.3°, 48.1°, and 54.9° corresponding to the (101), (200), and (211) planes, respectively, which indicates the TiO₂ anatase phase.⁷ These results confirm that the nanoparticles exist as TiO inside the CNFs

before activation, which is then converted to TiO_2 . The effective activation time for the conversion of TiO to TiO_2 lies between 10 and 30 min, indicated by the appearance of the 48.1° and 54.9° peaks during that period. The chemical state of the surface species of the composites is analyzed by X-ray photoelectron spectroscopy (XPS), and the $\text{Ti}2p$ spectra for ATCNF0 and ATCNF60 are shown in Figure 2b. Deconvolution of the ATCNF0 spectrum shows four peaks at 465.5, 461.3, 459.1, and 455.5 eV, corresponding to $\text{Ti}^{4+} 1/2$, $\text{Ti}^{2+} 1/2$, $\text{Ti}^{4+} 3/2$, and $\text{Ti}^{2+} 3/2$, respectively, which indicates that the nanoparticles on the surface of ATCNF0 are in TiO and TiO_2 forms.⁸ However, there are two peaks located at 459.1 and 465.5 eV, resulting from only TiO_2 , in ATCNF60

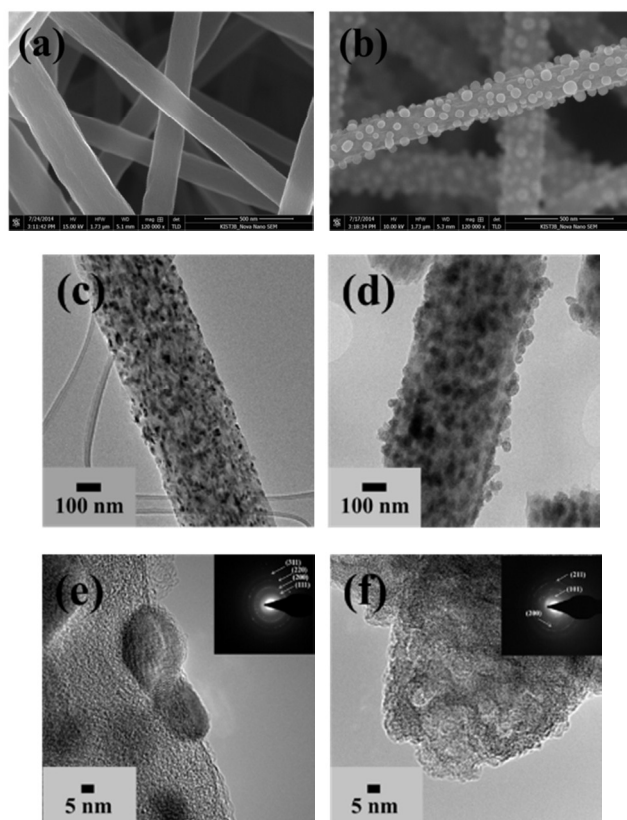


Figure 1 SEM images of (a) ATCNF0 and (b) ATCNF60, and TEM images of (c, e) ATCNF0 and (d, f) ATCNF60. Insets in (e) and (f) are SAED patterns of ATCNF0 and ATCNF60, respectively.

Structural evolution in the activation, as observed from micrographs, XRD, and XPS, suggests that oxygen draws the TiO nanoparticles from inside to the surface of the CNFs. Once on the surface, oxygen adsorbs to the nanoparticles, causing them to convert to TiO_2 , which is more thermodynamically stable than TiO . It is known that titanium isopropoxide reduces to TiO_2 during low-temperature sintering.⁹

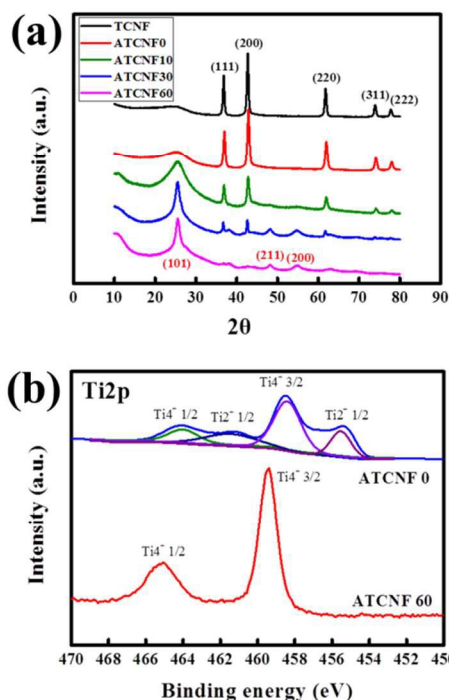


Figure 2 (a) XRD diffractograms of TCNF and its activated samples at various activation times, and (b) XPS $\text{Ti}2p$ spectra of ATCNF0 and ATCNF60.

However, it is likely that the carbonization of PAN under nitrogen do not result in the conversion to TiO_2 . Therefore, an additional oxidation is needed to obtain CNFs that contain TiO_2 nanoparticles. The surface segregation by adsorption of specific gases used as catalysts has been studied in metal composites as a method to control active sites and optimize their performance. Gao et al. reported that Pd layered with Au was segregated on the surface because of CO adsorption, which increased catalytically active sites.¹⁰ Although the composites used in this research are not bimetallic alloys, it is possible that a similar mechanism can be applied (Figure S3).

Table 1 – Textural properties of CNF, TCNF, and their activated samples (ACNF and ATCNF60)

Sample	S_{BET} (m^2/g)	Total pore volume (cm^3/g)	Average pore diameter (nm)
CNF	39.7	0.08	6.5
TCNF	100.3	0.16	6.3
ACNF	258.4	0.22	4.7
ATCNF60	436.0	0.35	4.5

As expected, the activation resulted in adsorption-induced growth of TiO_2 nanoparticles as well as a porous structure in the CNFs. The surface areas of pure CNF and TCNF are found to be 39.7 and 100.3 m^2/g , respectively, with a similar average pore diameter of ~ 6.5 nm. This phenomenon results from complex physical and chemical reactions, such as the reduction of the titanium isopropoxide and oxidation of the nanoparticles. After activation, a significant increase in the surface area is observed, where the values are 258.4 and 436.0 m^2/g for pure ACNF and ATCNF60, respectively (Table 1).

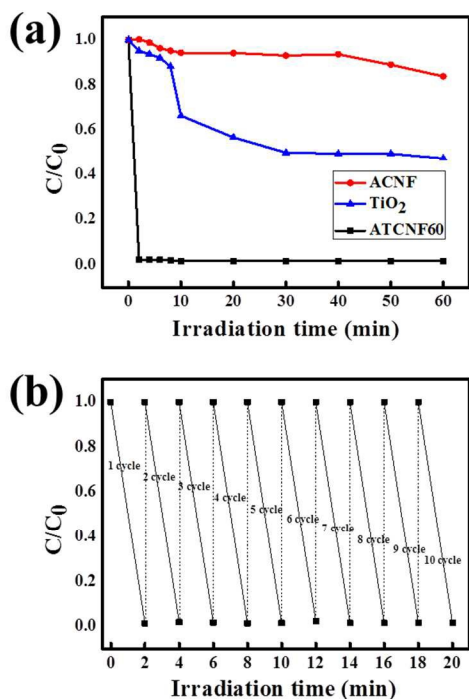


Figure 3 (a) Photo-catalytic degradation of MB as the concentration change versus irradiation time and (b) the cyclic performance of ATCNF60.

The photo-catalytic performance of commercial TiO_2 powder, pure ACNF, and ATCNF60 is evaluated by the methylene blue (MB) degradation test (Figure 3a). Although the pure ACNF reveals a porous structure, as determined from the BET measurement, only 10% of the MB degrades. Even TiO_2 powder does not degrade the MB completely for a UV exposure time of 60 min. However, MB is degraded completely within 2 min in the presence of ATCNF60, verifying that well-dispersed TiO_2 nanoparticles on the surface and partially exposed nanoparticles on the walls of the pores in the CNFs synergistically maximize photo-catalytic performance. To confirm the stability of ATCNF60, the cyclic test of MB degradation was carried out. Figure 3b showed the complete degradation of MB in 2 min over 10 cycles, indicating the stable photo-catalytic capability of ATCNF60. Note that conventional loading of TiO_2 particles by immersing activated carbon materials or stabilized PAN webs into a sol-gel solution can neither control the degree of dispersion nor maximize the surface area of activated carbon materials because of the blockage of pores by TiO_2 particles.^{3,5,11}

In conclusion, a simple method for synthesizing TiO_2 nanoparticle-loaded CNF webs has been demonstrated. PAN and titanium isopropoxide as precursors were physically mixed in dimethylformamide as solution dopes and were electrospun to prepare composite nanofiber webs. X-ray diffractograms and XPS spectra of resulting webs after stabilization and carbonization revealed TiO-related peaks and chemical bonding energies, respectively. An activation at 500 °C under an oxygen atmosphere converted TiO to TiO_2 , and aggregated

nanoparticles were well dispersed on the CNF surfaces by adsorption-induced surface segregation, as observed using SEM and TEM. Unlike the conventional synthesis of TiO_2 /carbon composites, PAN-based CNFs are used as substrates for nanoparticle loading, and only one-step activation is needed to produce well-dispersed TiO_2 nanoparticles on the surface of porous CNFs. The TiO_2 /CNF webs show the complete decomposition of MB in 2 min, indicating highly sensitive and fast-responding photocatalysts. It is probable that the synthesis can be utilized to control the size of TiO_2 nanoparticles and the surface morphologies of CNFs for synergetic effects on photocatalytic properties.

Acknowledgments

This work was supported by the Korea Institute of Science and Technology (KIST) Program.

Notes and references

^a Carbon Convergence Materials Research Center, Institute of Advanced Composite Materials, Korea Institute of Science and Technology, San 101 Eunha-ri, Bongdong-eup, Wanju-gun, Jeollabuk-do, 565-905, Republic of Korea.

^b Professional Graduate School of Flexible and Printable Electronics and Polymer Materials Fusion Research Center, Chonbuk National University, 664-14, Deokjin-dong, Deokjin-gu, Jeonju-si, Jeollabuk-do, 561-756, Republic of Korea.

^c Department of Nano Material Engineering, University of Science and Technology, Hwarangno 14-gil 5, Seongbuk-gu, Seoul 136-791 Republic of Korea.

Electronic Supplementary Information (ESI) available: details of experiments and results of SEM, XPS, textural properties. See DOI: 10.1039/c000000x/

- 1 B. O'Regan and M. Gratzel, *Nature*, 1991, **353**, 737
- 2 A. Hagfeldt and M. Gratzel, *Chem Rev*, 1995, **95**, 49
- 3 C.H. Kim, B.H Kim and K.S. Yang, *Carbon*, 2012, **50**, 2472
- 4 C. Wang, F. Jiang, R. Yue, H. Wang and Y. Du, *J Solid State Electrochem*, 2014, **18**, 515
- 5 ZC. Kadirova, Hojamberdiev, K-I. Katsumata, T. Isobe, N. Matsushita, A. Nakajima and K. Okada, *Environ Sci Pollut Res*, 2014, **21**, 4309
- 6 S. Yao, J. Li and Z. Shi, *Paticuology*, 2010, **8**, 272
- 7 G. Cui, W. Wang, M. Ma, M. Zhang, X. Xia, F. Han, X. Shi, Y. Zhao, Y. Dong and B. Tang, *Chem Commun*, 2013, **49**, 6415
- 8 M. Deqing and Y. DaiQi, *Surf Coat Tech*, 2009, **203**, 1154
- 9 R. Menzel, BF. Cottam, S. Ziemian, MSP. Shaffer, *J Matter Chem*, 2012, **22**, 12172
- 10 F. Gao, Y. Wang and DW. Goodman, *J Am Chem Soc*, 2009, **13**, 5734
- 11 J. Shi, J. Zheng, P. Wu and X. Ji, *Catal Commun*, 2008, **9**, 1846